ISSN: 2754-6675

Journal of Chemistry & its Applications

SCIENTIFIC Research and Community

Review Article

Open Access

Exploring a Dicationic Benzochromene with Dual photochromic and Electrochromic Response

De Azevedo ODCC*, Christopher DG, Mark HB, Paul AS and Jiangchun Wei

Department of Physical & Life Sciences, School of Applied Sciences, University of Huddersfield, Queensgate, Huddersfield, HD1 3DH, United Kingdom

ABSTRACT

This study reports the synthesis and characterization of the first dicationic 3,3diaryl-3H-benzo[f]chromene, substituted with pyridinium moieties at the C-8 position and the para-position of one of the C-3 aryl groups. The dicationic benzochromene and its precursors exhibit good photochromism with strong photocolourability in MeCN solutions. The neutral bispyridyl-substituted precursor transitions from colourless to orange (δPSS 452 nm) in solution upon UV irradiation, with a half-life (t1/2) of 812 s. Upon UV irradiation, the paleyellow dicationic benzochromene develops a deep orange hue in solution, accompanied by the formation of a broad absorption band with a shoulder around 460 nm, tailing to ca. 550 nm. The resulting photomerocyanine exhibits a shorter half-life (t1/2 = 522 s) compared to its neutral precursor. Spectroelectrochemical studies show that both the chromene form and the derived photomerocyanine of the dicationic benzochromene are electrochemically active, with reduction processes occurring at the pyridinium moieties. Upon applying a negative potential (−1.15 V to −1.35 V vs. Ag/AgCl) to the chromene form, a distinct strong absorption band at 520 nm emerges, indicative of the formation of a delocalized δ-radical species. The combined photochromic and electrochromic properties of the dicationic benzochromene highlight its distinct dual-functional behaviour, with different responses to both light and electrochemical stimuli.

***Corresponding author**

De Azevedo ODCC, Department of Physical & Life Sciences, School of Applied Sciences, University of Huddersfield, Queensgate, Huddersfield, HD1 3DH, United Kingdom.

Received: July 14, 2025; **Accepted:** July 24, 2025; **Published:** July 31, 2025

Keywords: Photochromism, Electrochromism, Viologen, Benzochromene, Cyclic Voltammetry

Introduction

Diarylpyran-derived photochromic systems have garnered significant attention over the years, primarily due to their commercialization in variable transmission optical devices, such as ophthalmic sun lenses [1-6]. Extensive structure–photochromic response relationships have been developed for isomeric naphthopyrans (benzochromenes) and related fused carbocyclic and heterocyclic systems (Figure 1) [7-9].

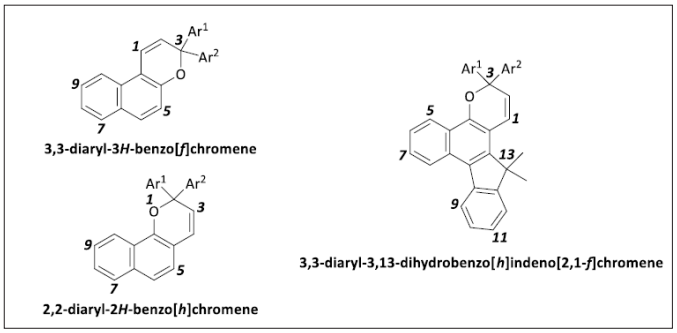

Figure 1: Selected Photochromic Benzo- and Indeno- Chromenes.

While many examples of neutral benzochromenes have been described over the decades, there is a limited number of examples featuring cationic substituents. Recent examples of cationic benzochromenes include the emissive Re(I)-complexes **1** described by De Azevedo et al., where the ^{3}MLCT (Metal-to-Ligand Charge Transfer) emission associated with the Re(I)centre could be photoswitched by cycling the appended photochromic benzochromene moiety (Figure 2) [10 a,b]. Studies on the metal complexation of various crown (e.g., **2**) and azacrown ether substituted benzochromenes (e.g., 3) by Fedorova *et al*., have led to a series of *in situ* generated cationic benzochromene systems that exhibited interesting responses to UV irradiation and assorted metal cations [11-14]. Triarylmethanol-appended benzochromenes (e.g., 4), which, upon treatment with acid, gave rise to cationic benzochromenes, have also been reported, where the hue of the dye cation was modulated by UV-initiated cycling of the pyran moiety [15,16]. The photocontrol of the emission of stilbazolium-substituted benzochromenes (e.g., 5) in polar media or mesoporous MCM-41 particles has also been reported [17].

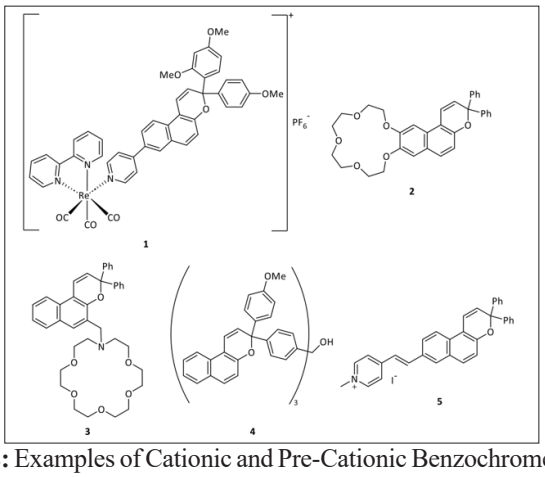

Figure 2: Examples of Cationic and Pre-Cationic Benzochromenes.

We have a longstanding interest in the synthesis and photochromic response of benzochromenes (naphthopyrans) [18-20] for a variety of variable transmission applications [21-22]. Recently, we decorated the periphery of a benzochromene unit with single pyridine units to generate a new series of photoswitchable ligands [10,23]. These works, combined with our established studies on electrochromic viologens and studies by others on pyridinium-substituted dithienylethenes, prompted us to explore the preparation of a dicationic pyridinium-substituted benzochromene 6 [24-27]. Our goal was to examine: (i) the influence of two cationic pyridinium units on the photochromic properties of the benzochromene system, and (ii) whether 6, in its ground state, exhibits an electrochromic response; and (iii) whether the T-type photochromic behaviour of the 3H- benzo[f]chromene unit, when interspersed between two terminal pyridinium units to form an extended viologen system 7, could enable the photomodulation of any potential electrochromic response (Scheme 1).

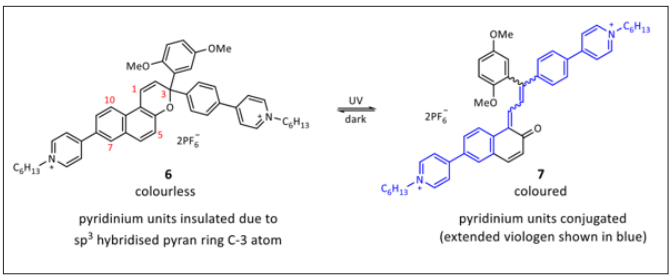

Scheme 1: Photoisomerization of the dicationic pyridinium-substituted benzochromene 6.

In relation to the previous aspect (iv), P-type photochromic dithienylethenes bearing terminal *N*-alkyl pyridinium units have been shown to exhibit interesting redox properties [28,29]. In a study concerning switchable molecular wires, Lehn *et al*., synthesized the dithienylethene 8 [26], which can be considered an extended viologen [30-32]. The authors demonstrated that 8 was essentially electrochemically inert; however, upon irradiation (365 nm), the ring closure of 8 to form the coloured isomer 9 was observed. A reversible one-electron reduction wave [half-wave potential of -0.23 V (vs. NHE/SCE/Ag)] was measured by cyclic voltammetry, indicating communication between the distant pyridinium termini (Scheme 2).

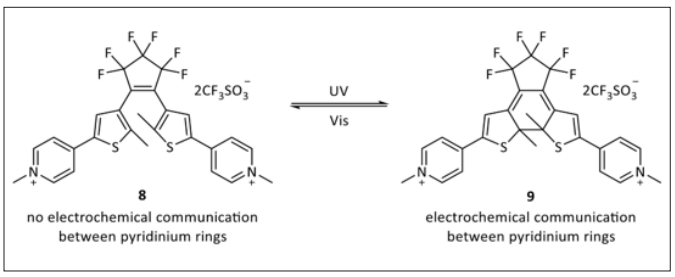

Scheme 2: Electrochemical Reaction of the Dithienylethene 8.

Discussion

The initial design of the dicationic benzochromene 6 embraced the commercial availability of 6-bromo-2-naphthol and the straightforward synthesis of (4-bromophenyl) (2,5dimethoxyphenyl) methanone 10 (Scheme 3). These building blocks introduce bromine atoms for further functionalization, while ketone 10 provides an electron-rich aryl ring in which one of the methoxy groups is located ortho to the C-3 atom of the pyran ring, a structural feature generally favouring the persistence of the ring-opened photomerocyanine [7,8,33].

(4-Bromophenyl) (2,5-dimethoxyphenyl) methanone 10 was obtained in moderate yield (39%) via direct Friedel-Crafts acylation of 1,4-dimethoxybenzene with 4-bromobenzoic acid in polyphosphoric acid at ca. 80 °C (Scheme 3). Transformation of 10 into propynol 11 was achieved in excellent yield (97%) by the addition of lithium (trimethylsilyl)acetylide (generated from n-BuLi and trimethylsilyl acetylene) to 10, followed by in situ base-mediated unmasking to provide the terminal acetylene. The acid-catalysed condensation of 11 with 6bromo-2-naphthol afforded dibromobenzochromene 12 in 73% yield. The structure of 12 was confirmed by NMR spectroscopy, with H-2 resonating as a doublet (J = 10.1 Hz) at □ 6.63, and C-3 appearing at □ 81.30, both features in full accord with literature data for structurally related compounds [7]. Suzuki cross-coupling of 12 with 4-(4,4,5,5-tetramethyl-1,3,2dioxaborolan-2-yl)pyridine was performed using our previously reported conditions, which prevent pyran ring contraction [34], affording a mixture of 8-(4-pyridyl)-benzochromene 13 (22%) and dipyridyl-substituted benzochromene 14 (29%); the latter was particularly challenging to elute from chromatography silica, even when using 40% MeOH in EtOAc. With 14 in hand, N-alkylation using excess 1-iodohexane proceeded smoothly in MeCN at reflux under protection from daylight. Isolation of the di-iodide salt was achieved by direct precipitation from the reaction mixture upon dilution with Et2O, followed by vacuum filtration. Iodide ion exchange using ammonium hexafluorophosphate in aqueous methanol (95%) completed the sequence, affording the dicationic benzochromene 6 as a pale-yellow powder in 67% yield over two steps. The ^{1}H NMR spectrum of 6 featured a multiple at δ 4.81 – 4.86 corresponding to the CH_2 units adjacent to the N^+ atoms, while H-2 appeared at δ 6.79 (1H, d, J = 10.1 Hz) and H-1 at δ 7.59 (1H, d, J = 10.1 Hz). The methoxy groups resonated as singlets at δ 3.60 and δ 3.78, while the protons ortho to the pyridinium N^+ centres were the most deshielded, appearing at δ 9.16 and δ 9.18. In the 13C{1H} NMR spectrum, C-3 appeared at δ 81.73, showing minimal shift despite the introduction of the dicationic pyridinium units. The incorporation of PF6- was confirmed by signals at δ -144.26 in the ^{31}P{^{1}H} NMR spectrum and δ -72.50 in the ^{19}F{^{1}H} NMR spectrum. High-resolution mass spectrometry confirmed excellent agreement between the measured and calculated species. A peak at m/z = 359.2062 corresponds to the dicationic complex $[M – 2(PF_6-)]^{2+}$, yielding an observed neutral mass of 718.4134 Da, which matches the calculated mass for $C_{49}H_{54}F_{12}N_2O_3P_2$ (mass error = 0.00 ppm). In addition, a peak at m/z = 863.3769 was observed, consistent with the monocationic ionpair [M – PF6-]+, indicating the presence of both dicationic and monocationic species under the ESI-MS conditions.

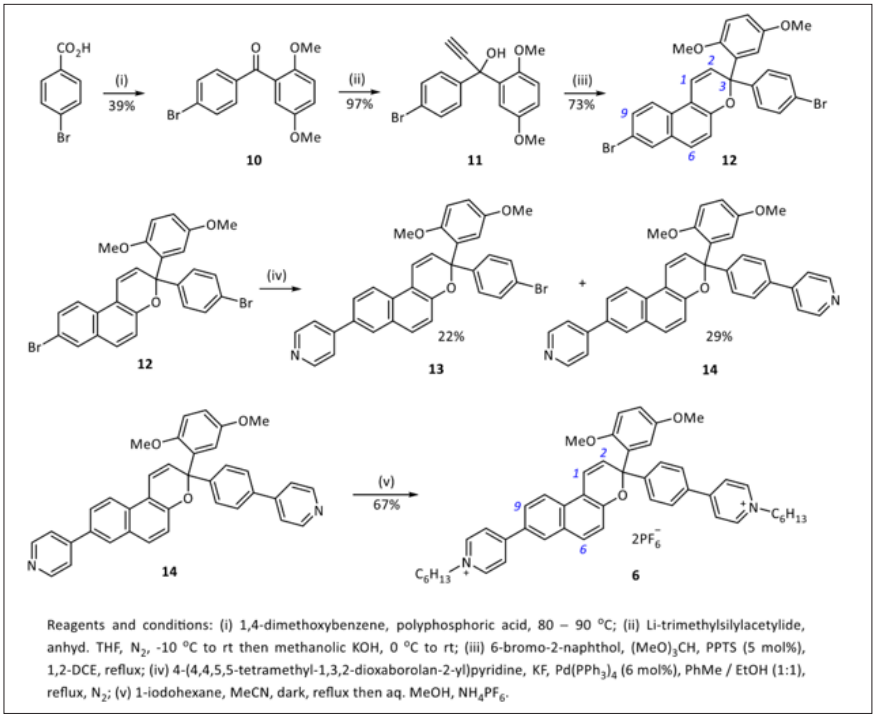

Scheme 3. Forward synthesis to the Dicationic Benzochromene 6.

The photochromic response of each of the neutral benzochromenes 12–14 in solution was next examined. In its ground state, dibromobenzochromene 12 displayed two overlapping UV-Vis absorption bands at 350 nm ($\delta = 3.6 \times 10^3$ $M^{-1}cm^{-1}$) and 364 nm ($\delta = 3.7 \times 10^3$ $M^{-1}cm^{1}$), with its acetonitrile solution appearing colourless (Figure 3). Upon UV irradiation, the solution quickly developed an orange hue, with a broad absorption peak emerging at 446 nm. The colour of the photostationary state faded following a bi-exponential decay function, with firstorder ($k\delta_1$) and second-order ($k\delta_2$) thermal bleaching rate constants of 3.4×10^{-2} s^{-1} and 8.6×10^{-4} s^{-1}, respectively, and a half-life (t1/2) of 727 s. The photocolourability factor (ΔAConc) was notably high at 1.2×10^4 M^{-1}, strongly influenced by the presence of the ortho-methoxy group on one of the aryl substituents at C-3. Upon excitation at 330 nm, no significant emission, apart from the Raman scattering artifacts of acetonitrile, was observed (Figure S46a).

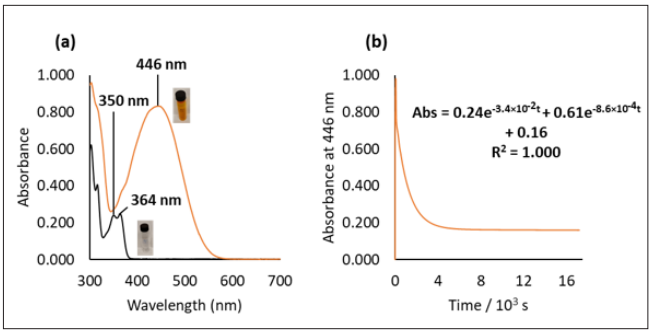

Figure 3: (a) UV-Vis absorption spectra of 12 before UV-irradiation (black) and after UVirradiation (orange, δ_{irr} 325 nm, 150 W) in aerated acetonitrile (0.067 mM) with inset images of acetonitrile solution in vials; (b) Thermal bleaching plot of 12 after UV-irradiation (δ_{irr} 325 nm, 150 W) to a photostationary state in aerated acetonitrile (0.067 mM).

A distinct pattern was observed for 8-(4-pyridyl)-benzochromene 13, which exhibited a single, broad UV-Vis absorption band at 361 nm ($\delta = 4.2 \times 10^3$ $M^{-1}cm^{-1}$) in its ground state (Fig 4). Like 12, its acetonitrile solution was initially colourless but turned orange upon UV exposure, with a broad absorption band at 446 nm. The colour of the photostationary state bleached following a typical bi-exponential decay function, with $k\delta_1$ and $k\delta_2$ equal to 1.0×10^{-3} s^{-1} and 5.2×10^{-5} s^{-1}, respectively, with a t1/2 of 595 s. Similar to 12, the photocolourability factor (ΔAConc) was high at 1.4×10^4 M^{-1}. However, unlike 12, excitation at 330 nm resulted in a distinct emission band at 394 nm, likely arising from a singlet excited state with significant intramolecular charge-transfer (ICT) character from the naphthopyran to the pyridyl unit (1ICT, NP → Py) (Figure S46b).

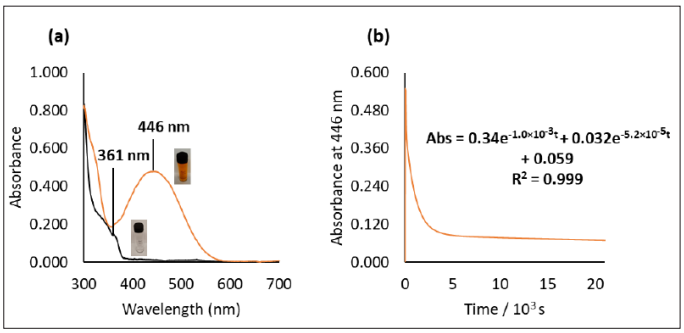

Figure 4: (a) UV-Vis absorption spectra of 13 before UV-irradiation (black) and after UVirradiation (orange, δ_{irr} 325 nm, 150 W) in aerated acetonitrile (0.035 mM) with inset images of acetonitrile solution in vials; (b) Thermal bleaching plot of 13 after UV-irradiation (δ_{irr} 325 nm, 150 W) to a photostationary state in aerated acetonitrile (0.035 mM).

Dipyridyl-substituted benzochromene 14 also featured a broad absorption band at 361 nm ($\delta = 3.6 \times 10^3$ $M^{-1}cm^{-1}$) in its ground state, with an initially colourless solution that developed an orange hue under UV irradiation (Fig. 5). The photoinduced absorption band of 14 was slightly redshifted, with a peak at 452 nm. The colour of the photostationary state bleached following a bi-exponential decay function, with $k\delta_1$ and $k\delta$ equal to 9.1 × 10^{-4} s^{-1} and 9.7×10^{-5} s^{-1}, respectively, with a t1/2 of 812 s. The

photocolourability factor (ΔAConc) was equally high at 1.5×10^4 M^{-1}. The emission profile closely resembled that of 13, featuring an emission band with ICT character from the naphthopyran to the pyridyl unit (1ICT, NP → Py) at 393 nm (Figure S46c).

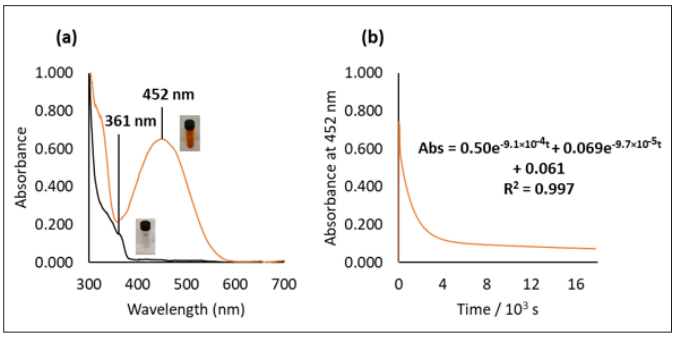

Figure 5: (a) UV-Vis absorption spectra of 14 before UV-irradiation (black) and after UVirradiation (orange, δ_{irr} 325 nm, 150 W) in aerated acetonitrile (0.043 mM) with inset images of acetonitrile solution in vials; (b) Thermal bleaching plot of 14 after UV-irradiation (δ_{irr} 325 nm, 150 W) to a photostationary state in aerated acetonitrile (0.043 mM).

The fatigue resistance plots of benzochromenes 12–14 after four irradiation–bleaching cycles are shown in Fig. 6. For compounds 12 and 13, there was an initial decrease in the maximum absorbance after the first irradiation cycle, but subsequent cycles showed little to no decrease in absorbance. In contrast, compound 14 exhibited gradual fatigue with each irradiation cycle, suggesting that the introduction of the electron-withdrawing 4-pyridylphenyl group at C-3 may be accelerating photodecomposition. Previously, we noted that highly electron-deficient gem-aryl groups at C-3 in 3*H*-benzo[*f*]chromenes can cause ring contraction to a benzofuran structure, disrupting normal photochromic cycling and resulting in a loss of photochromism [35]. This process may be occurring in 14. Additionally, we have observed poor fatigue resistance in 3-phenyl-3-(4-pyridyl)-3*H*-naphtho[2,1-b]pyran, where the electronwithdrawing 4-pyridyl group is directly bonded to C-3 of the pyran ring [23]. Furthermore, colour bleaching, in addition to occurring thermally, was assisted by irradiation with visible light, revealing the mixed P- and T-type photochromic character of compounds 12–14.

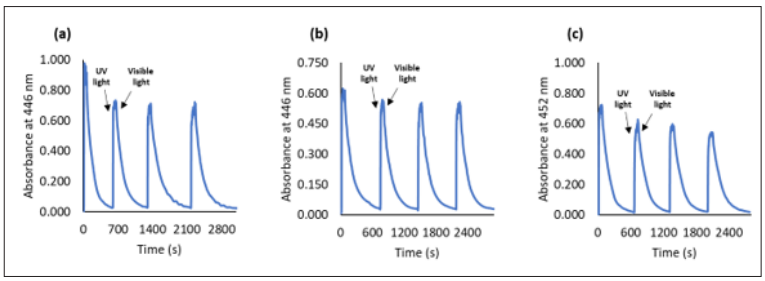

Figure 6: Irradiation – bleaching cycles for (a) an aerated acetonitrile solution (0.067 mM) of 12; (b) aerated acetonitrile solution (0.035 mM) of 13; (c) an aerated acetonitrile solution (0.043 mM) of 14.

The UV-Vis absorption spectrum of bispyridinium salt 6 in its ground state showed a single absorption band at 386 nm (δ = 1.5 × 104 M-1cm-1), extending into the visible region. Consequently, its acetonitrile solution appeared pale yellow (Fig. 7, Table 1). Upon UV irradiation, the solution rapidly turned deep orange, displaying a new absorption shoulder at 460 nm that extended further into the visible region, although no distinct maximum absorption was observed at the photostationary state (δ_{PSS}). The colour of the photostationary state faded following a bi-exponential decay, with rate constants $k\delta_1$ = 1.7 × 10-3 s-1 and $k\delta_2 = 2.9 \times 10^{-5}$ s^{-1}, and a half-life (t1/2) of 522 s. The photocolourability factor (δAConc) for 6 was 8.5×10^3 M^{-1}.

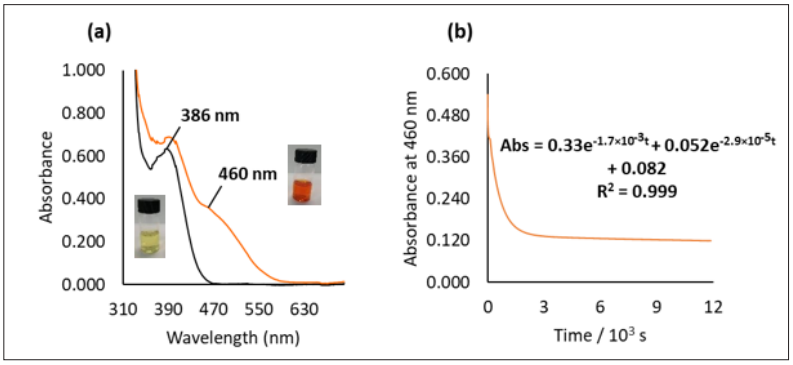

Figure 7: (a) UV-Vis Absorption Spectra of 6 Before UV-irradiation (black) and after UVirradiation (deep orange, δ_{irr} 325 nm, 150 W) in aerated acetonitrile (0.042 mM) with inset images of acetonitrile solution in vials; (b) Thermal bleaching plot of 6 after UV-irradiation (δ_{irr} 325 nm, 150 W) to a photostationary state in aerated acetonitrile (0.042 mM).

The fatigue of dicationic benzochromene 6 was investigated in a CD3CN solution using 1H NMR spectroscopy (Figure 8). Irradiation of an NMR tube containing the solution of 6 was performed with a low-power LED UV flashlight (δ_{irr} 365 nm, 2 watt) placed in contact with the NMR tube. 1H NMR spectra were recorded after specific irradiation times. After 20 minutes of irradiation, the sample was allowed to relax for 10 minutes before acquiring the 1H NMR spectrum. While the sample appeared unaffected after 120 minutes of continuous irradiation, significant degradation was evident in the 1H NMR spectrum after just 8 hours of irradiation.

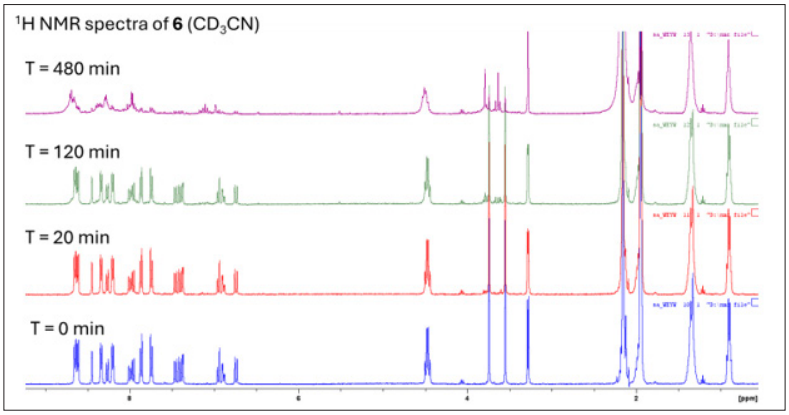

Figure 8: Stacked ^{1}H NMR spectra of 6 (CD3CN) recorded after 0, 20, 120, and 480 min of UV irradiation (LED portable UV flashlight, δ_{irr} 365 nm, 2 watt).

A preliminary survey of the emission properties of 6 revealed that, upon excitation at 390 nm, an emission band centred at 577 nm was observed in aerated acetonitrile (Fig. S47), corresponding to an excitation band at 388 nm (Stokes shift of 189 nm), which aligned well with the absorption band at 386 nm. A very similar emission band at 570 nm was also recorded in aqueous MeOH (Fig. S48). Hexylation of 14 to give 6 led to a significant bathochromic shift of 184 nm in the emission band in aerated acetonitrile (Fig. S49). The emissive event exhibited a very short lifetime, with three components of 0.16 ns (τ_1), 0.55 ns (τ_2), and 3.02 ns (τ_3).

A comparison of the photochromic response of dibromobenzochromene 12 with that of 8-(4pyridyl)-benzochromene 13 revealed that the replacement of the 8-Br atom with an 8-(4pyridyl) unit has negligible effects on both δPSS and ΔAConc. However, the rate of thermal bleaching decreased with the introduction of the pyridyl group at C-8; a similar phenomenon was noted for mono-pyridyl substituted benzochromenes. The $k\delta_1$ and $k\delta_2$ values decreased from 3.4×10^{-2} s^{-1} and 8.6×10^{-4} s^{-1}, respectively, for 12, to 1.0×10^{-3} s^{-1} and 5.2×10^{-5} s^{-1}, respectively, for 13. The half-lives (t1/2) of 12 (727 s) and 13 (595 s) do not reflect the decrease in the rate of thermal bleaching due to variations in the populations of the transoid-cis (TC) and transoid-trans (TT) isomers, as these are a function of the irradiation time, among other factors, which is reflected by the different amplitude values in the rate equations. Literature examination reveals that the incorporation of donor groups, such as alkoxy (MeO) or secondary amino (4-methylpiperaz-1-yl) groups at the 8-position in 3H-benzo[f]chromenes results in an appreciable bathochromic shift of absorbance of about 40–80 nm [36]. On the other hand, extending conjugation at C-8 with a phenyl group results in a smaller bathochromic shift (30 nm) in the δPSS of the photomerocyanine [37]. Previous work on the decoration of the periphery of the 3H-naphtho[2,1-b] pyran ring system with pyridyl substituents reveals only an 11 nm bathochromic shift in the δPSS upon the introduction of a 4-pyridyl unit at C-8, relative to the absorption maximum of the unsubstituted parent compound [23]. It is likely that the 4-pyridyl moiety in 13 exhibits a similar electronwithdrawing effect to the Br substituent in 12 when located at C-8 in the 3H-naphtho[2,1b] pyran moiety. The incorporation of the second pyridine nucleus to generate dipyridylsubstituted benzochromene 14 resulted in a small (6 nm) bathochromic shift in the δPSS of the associated photomerocyanine relative to those derived from 12 and 13. Once again, no significant changes were observed in δAConc when comparing 14 with 12 and 13. A more noticeable change was the significant increase in the persistence of the photomerocyanine of 14. Although there was an increase in $k\delta_2$ from 5.2×10^{-5} s^{-1} (13) to 9.7×10^{-5} s^{-1} (14), there was a decrease of 11% in $k\delta_1$ for 14 ($k\delta_1 = 9.1 \times 10^{-4}$ s^{-1}) compared to 13 ($k\delta_1 = 1.0 \times 10^{-3}$ s^{-1}). As a result, the half-life (t1/2) increased from 595 s (13) to 812 s (14). The incorporation of electron-withdrawing groups, such as fluorine atoms, into the gem-diaryl unit of 3Hbenzo[f]chromenes is generally associated with bathochromic shifts in the absorption maxima and increased persistence of the photomerocyanines. However, in this current study, there is a conflict between the electron-withdrawing character of the pyridyl moiety and the extended conjugation it imparts in the photomerocyanine, with the net result being a 6 nm bathochromic shift.

N-Alkylation of the pyridine N-atoms of 14 resulted in dicationic benzochromene 6, which exhibited an absorption maximum of the ring-closed pyran form (δmax 386 nm), bathochromically shifted by 20 nm relative to the pyran forms of 12–14. As a consequence of this longer UV-absorption wavelength, 6 appeared pale yellow, and the photomerocyanine 7, with a shoulder band at 460 nm upon UV irradiation overlapping with the shorter wavelength absorbing UV band, appeared deep orange. It is noteworthy that the δAConc of 6 (δAConc = 8.5×10^3 M^{-1}) was reduced by 43% compared to 14 (δAConc = 1.5×10^4 M^{-1}). Additionally, there was a noticeable decrease in the persistence of the photomerocyanine of 6 as a result of the N-alkylation of 14. Despite the decrease in $k\delta_2$ from 9.7×10^{-5} s^{-1} (14) to 2.9×10^{-5} s^{-1} (6), there was an increase of 87% in $k\delta_1$ for 6 ($k\delta_1 = 1.7 \times 10^{-3}$ s^{-1}) compared to 14 ($k\delta_1 = 9.1 \times 10^{-4}$ s-1), which ultimately led to a decrease in the half-life (t1/2) from 812 s (14) to 522 s (6). In addition to their photochromic response, a preliminary survey of the emission properties of benzochromenes 12 – 14 and 6 was conducted. Benzochromenes 13 and 14 exhibited fluorescence in the long-wavelength UV region, with broad emission bands at approximately 395 nm. These emissions are likely of ^{1}ICT (NP → Py) character, a feature previously observed in mono-pyridyl-substituted benzochromenes [10b, 23], and arise directly from the introduction of a 4-pyridyl group at C-8. In contrast, 12 was virtually non-emissive. Bipyridinium salt 6 displayed fluorescence in both aerated MeCN and aqueous MeOH, with δem at 577 nm and 570 nm, respectively, and a very short lifetime, consistent with emission from a singlet excited state. Although the exact reason for the bathochromic shift in δem relative to 14 remains unclear, alkylation of the pyridyl group to form a pyridinium likely enhances its electron-withdrawing nature. This increased electron deficiency is expected to stabilize (i.e., lower) the LUMO energy, thereby reducing the HOMO–LUMO gap – leading to the observed red shift in emission.

Table 1: Summary of the Spectroscopic Data of Photochromes 12 – 14 and 6 and Respective Photomerocyanines obtained after Continuous UV-Irradiation (δ_{irr} 365 nm, 150 W) to a Photostationary State (PSS) in Aerated Acetonitrile Solution.

Target	δ_{max} [a] / nm	δ_{PSS} [c] / nm	δA_{Conc} [d] / M^{-1}	kδ [e] / s^{-1}	t1/2 [f] / s
	(ε [b] / $M^{-1}cm^{-1}$)			(Amplitude / %)	
12	350 (3.6 × 10^3)	446	1.2 × 10^4	3.4 × 10^{-2} (28) [kδ_1]	727
	364 (3.7 × 10^3)			8.6 × 10^{-4} (72) [kδ_2]	
13	361 (4.2 × 10^3)	446	1.4 × 10^4	1.0 × 10^{-3} (91) [kδ_1]	595
				5.2 × 10^{-5} (9) [kδ_2]	
14	361 (3.6 × 10^3)	452	1.5 × 10^4	9.1 × 10^{-4} (88) [kδ_1]	812
				9.7 × 10^{-5} (12) [kδ_2]	
6	386 (1.5 × 10^4)	460 (shoulder band)	8.5 × 10^3	1.7 × 10^{-3} (86) [kδ_1]	522
				2.9 × 10^{-5} (14) [kδ_2]	

[a]δ_{max} = maximum wavelength of absorption at the ground state. [b]δ = molar extinction coefficient. [c]δ_{PSS} = maximum wavelength of absorption at the photostationary state (PSS). [d] δA_{Conc} = colour generated at the photostationary state (PSS) after continuous UV-irradiation of 1 molar of a given naphthopyran in solution, calculated as δA / Conc, with δA being the induced optical density at δPSS and Conc the concentration of the naphthopyran in solution prior to UV-irradiation. e kδ = thermal bleaching rate constant. *f* $t1/2$ = time in seconds required for the sample to return to half the optical density at the Photostationary State (PSS).

Our attention next turned to an electrochemical study to determine whether: (i) dicationic benzochromene 6 in its ground state exhibits an electrochromic response, and (ii) electronic communication occurs between the two pyridinium termini in the photomerocyanine 7. As expected, 6 was electrochemically active in MeCN solution, as shown by its cyclic voltammograms (Fig. 9). It exhibited two closely spaced oxidation processes: the first [E_{ox1} = +0.96 V *vs*. Fc (+1.66 V *vs*. SHE)] was irreversible, while the second [E_{ox2} = +1.06 V *vs*. Fc (+1.76 V *vs*. SHE)] was quasi-reversible to nearly fully reversible. In the reduction sweep, a clear irreversible reduction process was observed at E_{red1} = -1.58 V vs. Fc (-0.88 V *vs*. SHE), attributed to electron acceptance by a pyridinium moiety. A second, poorly defined, irreversible reduction appeared at E_{red2} = -1.85 V vs. Fc (-1.15 V vs. SHE), likely due to the reduction of a second pyridinium moiety. The observation of two distinct reduction waves suggests minimal electronic communication between the pyridinium termini in the ground state, as would be expected given their spatial separation and the cross-conjugated chromophore.

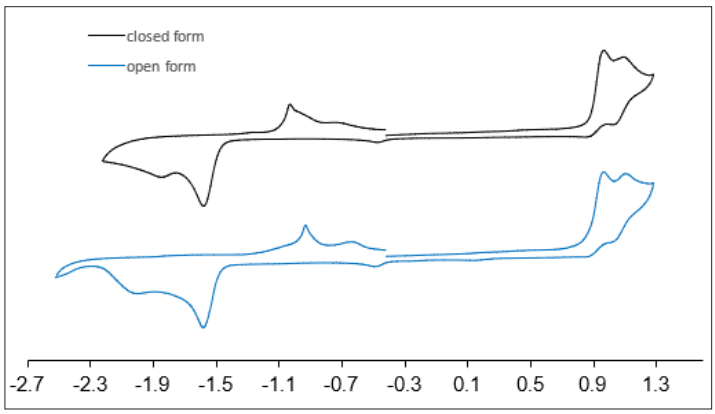

Figure 9: Cyclic voltammograms recorded at 100 mVs^{-1} for a 2 mM MeCN solution of salt 6 [prior to UV irradiation, black voltammogram and post continuous UV irradiation (δ_{irr} 365 nm, 2 W) for 300 s, blue voltammogram]. Potentials are quoted relative to the Fc+/Fc couple.

Irradiation of 6 at 365 nm induced a distinct colour change from pale yellow to deep orange, corresponding to the formation of photomerocyanine 7. The oxidation processes [E_{ox1} = +0.96 V vs. Fc (+1.66 V vs. SHE), irreversible; E_{ox2} = +1.06 V vs. Fc (+1.76 V vs. SHE)] and the first reduction [E_{red1} = -1.58 V vs. Fc (-0.88 V vs. SHE), irreversible] remained unchanged (Fig. 9), indicating they occur at molecular sites unaffected by the photoinduced ring-opening process. However, the second reduction of photomerocyanine 7 underwent a slight cathodic shift by 0.16 V to E_{red2} = -2.01 V vs. Fc (-1.31 V vs. SHE), suggesting an altered electronic structure upon photoinduced transformation.

For comparison, the first and second reduction potentials of simple methyl viologen chloride 15 are reported as -0.45 V and -0.88 V vs. SHE in water [39]. The furan-separated viologen fluoroborate 16 exhibits Ered1 = -0.50 V and E_{red2} = -0.69 V in MeCN (corrected to SHE), while thiophene-separated viologen fluoroborate salts 17 show reductions at -0.45 V and -0.60 V in MeCN (corrected to SHE) [40]. The vinyl-separated viologen 18 has been reported to have Ered1 = -0.28 V and E_{red2} = -0.47 V (MeCN, corrected to SHE) [41]. Interestingly, the 1,4phenylene-spaced viologen 19 and divinyl analogue 20 each exhibit a single two-electron reduction at -0.67 V and -0.35 V (MeCN, corrected to SHE), respectively (Fig. 10) [40]. The 1methyl-4-phenylpyridinium salt 21 has been reported to have Ered1 = -1.19 V (MeCN, corrected to SHE) [42].

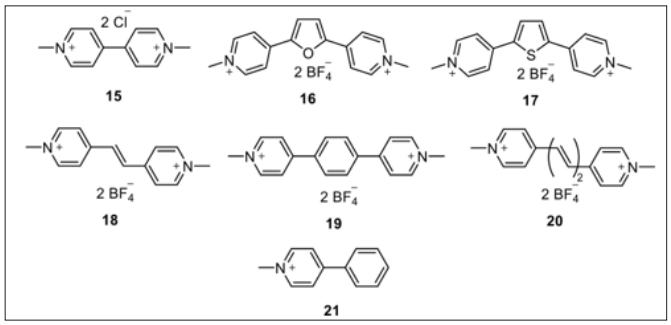

Figure 10: Representative Examples of Viologen and Viologen-like Systems.

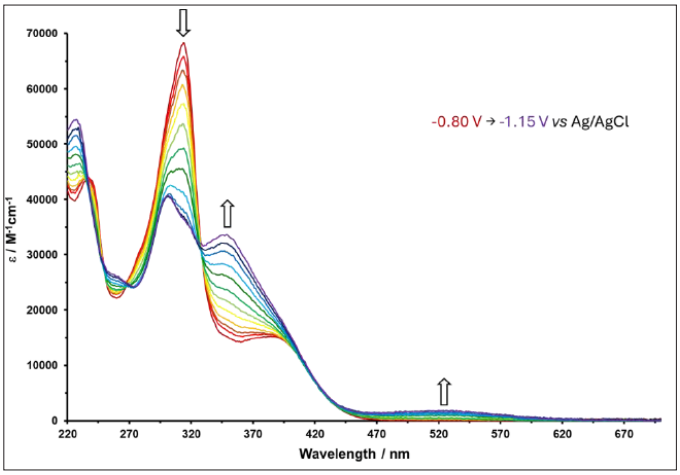

Figure 11: Absorption spectra of 6 in MeCN under an applied voltage range from -0.8 to -1.15 V (vs. Ag/AgCl).

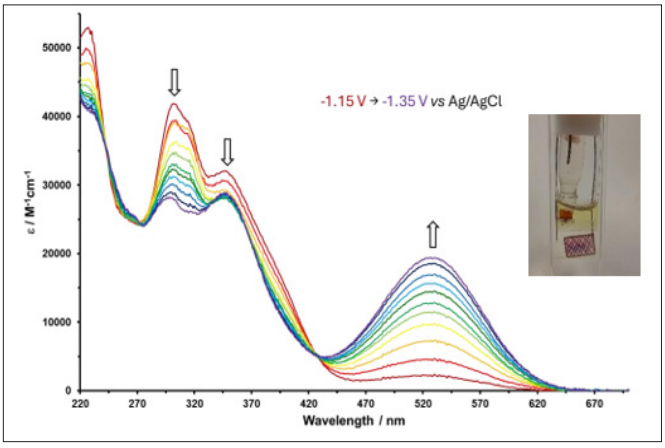

Figure 12: Absorption Spectra of 6 in MeCN Under an Applied Voltage Range from -1.15 to -1.35 V (vs. Ag/AgCl), (image of spectroelectrochemical cell insert).

The emergence of a broad absorption band at approximately 520 nm upon application of a negative potential to a MeCN solution of 6 warrants further discussion (Fig. 11 and 12). Within the applied potential range [-0.80 V to -1.35 V vs. Ag/AgCl (ca. -0.6 V to -1.1 V vs. SHE)], it is reasonable to expect that both pyridinium units undergo reduction, initially forming either the monoradical cationic intermediates 22 or 23, and subsequently generating the diradical species 24 (Figure 13). A comparison with literature data on spectroelectrochemical studies of viologen systems provides insight into the nature of this absorption (Figure 14). Delocalized δmonoradical cations derived from the electrochemical reduction of compounds 16 and 17 exhibit absorption maxima in the visible region at 561 nm and 568 nm, respectively [40]. Additionally, the bis-N-hexyl analogue of 19, compound 25, displays an absorption maximum at 556 nm in propylene carbonate, while the 2,6-naphthyl-separated viologen 26 [43] and the triphenylpyridinium salt 27 [44] exhibit maxima at 636 nm (propylene carbonate) and 581 nm (MeCN), respectively. This comparison suggests that the broad band observed at 520 nm for 6 arises from a delocalized electronic structure in its reduced state.

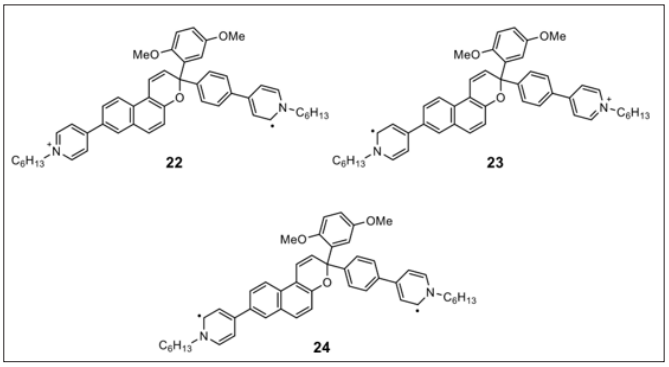

Figure 13: Proposed Intermediates (Delocalisation not shown) resulting from Electrochemical Reduction of 6.

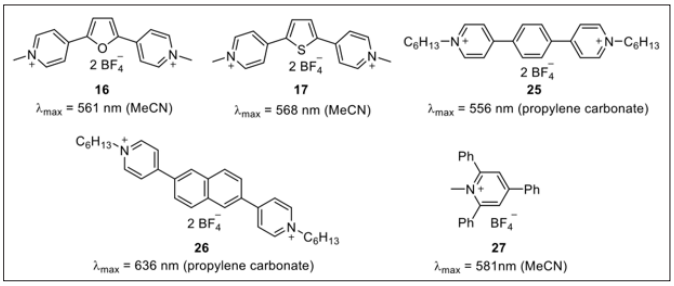

Figure 14: Visible Absorption Maxima of Radical Cations derived from Extended Viologen Systems.

While the electrochemistry of diaryl-substituted benzochromenes has yet to be explored, spiropyrans have received notable attention in this regard (Scheme 4). Specifically, spiropyrans 28 and 29 have been reported to undergo ring-opening upon one-electron oxidation [45,46]. Unfortunately, no absorption data were reported for the resulting ringopened species 30, though electron spin resonance (ESR) spectra confirmed the formation of the di-tert-butylphenoxyl radical. In contrast, detailed spectroelectrochemical studies have been conducted on 31, where oxidation at 1.3 V vs. SCE led to the appearance of a broadened absorption band centred at approximately 460 nm in MeCN (0.1 M TBA PF6). Furthermore, oxidation of the related di-tert-butyl-substituted spiropyran 32 at 1.0 V (0.1 M TBA PF6) resulted in the formation of the coloured radical cation 33, characterized by absorption maxima at 355 nm and 505 nm [47]. These studies highlight the propensity of spiropyran derivatives to undergo electrochemically induced ring-opening, generating highly coloured radical cationic species.

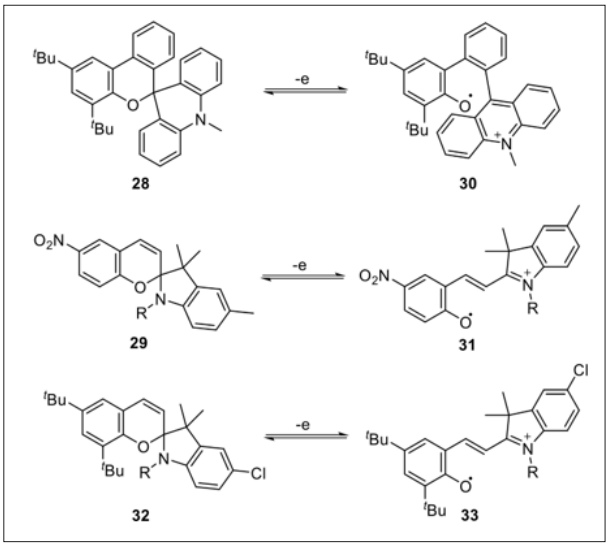

Scheme 4: Electrochemical (oxidative) Ring-Opening of Spiropyrans.

The emergence of a broad absorption band centred at 520 nm upon application of a negative potential to a MeCN solution of 6 raises intriguing questions regarding the electronic and structural changes occurring upon reduction. Given the established behaviour of viologen derivatives, this absorption feature suggests evident δ-system delocalization in the diradical species. However, it is worth considering whether additional structural transformations, such as ring-opening, could be contributing to the observed spectral changes. While there is currently no direct evidence supporting a ring-opening transformation in 6 (Scheme 5), the comparison with related systems offers a compelling basis for further exploration. The electrochemical behaviour of spiropyrans, which are structurally distinct but mechanistically relevant, provides a precedent for electrochemically induced ring-opening. Spiropyrans 28 and 29, for instance, undergo one-electron oxidation, triggering structural rearrangement and leading to the formation of open-ring radical species. Moreover, the oxidation of di-tert-butylsubstituted spiropyran 32 results in the radical cation 33, which exhibits absorption bands at 355 nm and 505 nm – values not very different from the absorption bands observed for reduced 6. Given these precedents and the distinct electrochemical properties of 6, further investigation into this hypothesis would be valuable. Future studies using electron paramagnetic resonance (EPR) spectroscopy and computational modelling could help determine whether an electrochemically induced ring-opening occurs. If confirmed, this would distinguish 6 from conventional viologen-based compounds, offering new mechanistic insights into its redox behaviour and potential applications. However, a more comprehensive spectroscopic and electrochemical investigation is necessary to further explore and validate the preliminary data presented in this study.

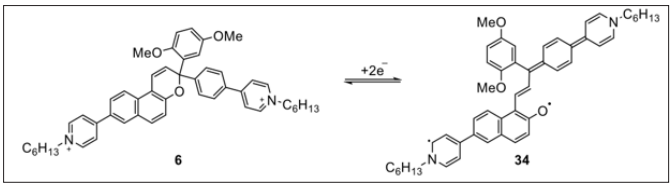

Scheme 5: Hypothetical electrochromic ring-opening of dicationic benzochromene 6 (delocalisation not shown).

To assess whether 6 functions as a reversible electrochrome, we must examine its reduction sweep. The first reduction (Ered1) was irreversible, suggesting that once 6 accepts an electron, the resulting radical species does not readily revert to the original state under standard electrochemical conditions. The second reduction (Ered2) was also irreversible, further indicating that full electrochemical reversibility is not achieved. For a material to be considered a fully reversible electrochrome, the redox processes should ideally be quasireversible or fully reversible, allowing for efficient switching between states over multiple cycles. While 6 does exhibit electrochromic behaviour, the irreversibility of its reduction steps suggests that the radical species formed upon reduction undergo structural or chemical changes that prevent efficient reoxidation. This may lead to progressive degradation of its electrochromic response over multiple switching cycles, limiting its potential as a fully reversible electrochromic material. Nonetheless, its electrochromic behaviour remains of interest, offering valuable insights into the relationship between molecular structure and reversibility that may be leveraged to develop enhanced electrochromic benzochromene dyes.

We also attempted the challenging task of conducting a spectroelectrochemical investigation of the ring-opened species 7. This experiment was technically complex because 6 had to be continuously UV irradiated during the measurements to maintain a photostationary state containing photomerocyanine 7. To achieve this, an MeCN solution of 6 was irradiated with a LED UV flashlight (δ_{irr} 365 nm, 2 watt) for 12 minutes in a spectroelectrochemical cell, yielding a deep orange solution consistent with the formation of a significant amount of 7. Applying a potential sweep from -0.80 V to -0.90 V vs. Ag/AgCl (-0.6 V to -0.7 V vs. SHE) while maintaining UV irradiation led to a decrease in absorption in the visible region (Fig. 15). Extending the potential range further to -0.90 V to -1.15 V vs. Ag/AgCl (-0.7 V to -0.9 V vs. SHE) induced additional spectral changes (Fig. 16), most notably the emergence of a new absorption band centred at ca. 360 nm, likely corresponding to the formation of an electronically localized radical.

As discussed earlier by cyclic voltammetry, the oxidation processes [Eox1 = +0.96 V vs. Fc (+1.66 V vs. SHE), Eox2 = +1.06 V vs. Fc (+1.76 V vs. SHE)] and the first reduction [Ered1 = -1.58 V vs. Fc (-0.88 V vs. SHE)] remained unchanged upon photochromic reaction. Only the second reduction of photomerocyanine 7 underwent a slight cathodic shift by 0.16 V to Ered2 = -2.01 V vs. Fc (-1.31 V vs. SHE), irreversible, indicating some modification of the electronic structure upon photoinduced transformation. The

small cathodic shift in Ered2 suggests that photochromism does influence the electrochemical properties of 7, but only to a limited extent. If photomodulation strongly impacted electrochromism, we would expect more substantial changes in both the reduction/oxidation potentials and the spectral behaviour resulting from the photochromic reaction. The lack of significant photomodulation implies minimal to negligible electronic communication between the two pyridinium moieties, leading to largely independent redox processes at each site. Furthermore, the relatively high Ered values in 7 suggest that reduction is less favourable compared to conventional viologens. This could be attributed to the weak electronic coupling between the pyridinium units, which prevents efficient charge delocalization and stabilization of the reduced species. Unlike classic viologens, where reduction leads to a delocalized radical state, 7 instead appears to form an electronically localized species upon reduction, further supporting the notion that the pyridinium termini do not effectively communicate.

Interestingly, the reduction sweep of 7 led to a rapid decrease in the 460 nm absorption band – a much faster spectral response than observed during thermal bleaching under similar conditions. While a direct comparison of rates between spectroelectrochemical and thermal processes is complicated by differing experimental factors, this observation suggests that radical formation in 7 disrupts, rather than extends, the existing δ-conjugation, unexpectedly yielding a spectrum similar to that observed after the first pyridinium reduction of 6. While this spectral resemblance might imply a direct ring-closing event, it could also reflect analogous electronic changes in both processes, driven by the formation of an electronically localized radical rather than complete structural reversion.

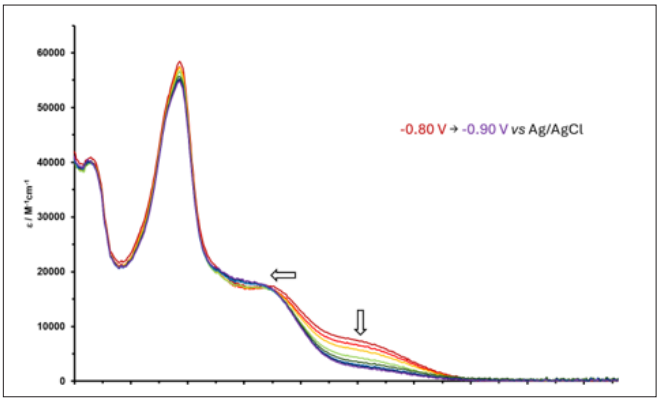

Figure 15: Absorption Spectra of 7 in MeCN under an Applied Voltage Range from -0.80 to -0.90 V (vs. Ag/AgCl).

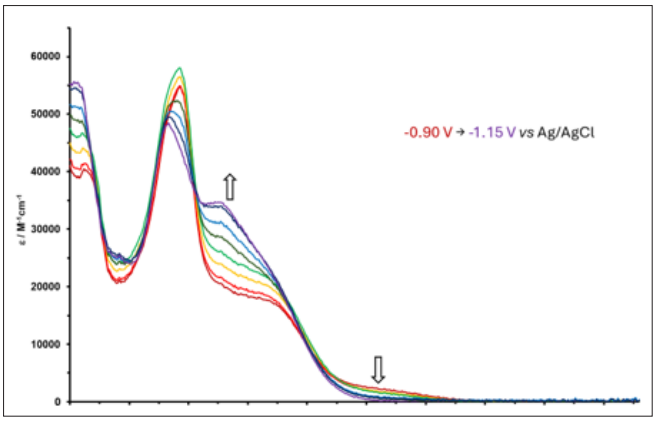

Figure 16: Absorption spectra of 7 in MeCN under an applied voltage range from -0.90 to -1.15 V (vs. Ag/AgCl).

Conclusions

This study reports the synthesis of the first dicationic benzochromene (6) via a three-step reaction sequence. The process involves the acid-catalysed condensation of a 2-naphthol with a 1,1-diarylprop-2-yn-1-ol, followed by Suzuki cross-coupling to introduce the pyridine units, and concluding with N-alkylation and counterion exchange, affording 6 in an overall yield of 14%.

The photochromism of 6 in MeCN solution is evident from the reversible development of an orange hue upon UV irradiation, accompanied by a broad absorption feature centred around 460 nm and a half-life (t1/2) of 522 s. Compared to the neutral bispyridyl precursor 14 (δPSS 452 nm, $t_{1/2}$ = 812 s), 6 exhibits a marginally red-shifted absorption and a significantly shorter half-life.

A preliminary survey of the emission properties of the benzochromenes reveals that 6 exhibits significantly red-shifted fluorescence (by 184 nm) compared to its neutral precursor 14, with emission maxima at 577 nm in MeCN and 570 nm in aqueous MeOH.

Electrochemical studies reveal that 6 also displays electrochromic behaviour, with the development of a red-coloured species (δ_{max} = 520 nm) upon electrochemical reduction of the pyridinium moieties. This process suggests the formation of an electronically delocalized diradical species, potentially linked to an electrochemically triggered pyran ring-opening transformation as a consequence of the presence of the red-ox active pyridyl substituents. While tentative, this would contrast with the oxidative ring-opening observed in spiropyrans 28, 29 and 32, highlighting the possibility of divergent redox-induced pathways across these photochromic systems.

Cyclic voltammetry shows that three redox processes – E_{ox1}, E_{ox2}, and E_{red1} – remain unchanged upon the photochromic reaction to generate photomerocyanine 7, suggesting that oxidation and the first reduction occur at unaffected sites. However, the second reduction of photomerocyanine 7 exhibits a slight cathodic shift, indicating a minor modification in the electronic structure. This small shift in Ered2 suggests limited photomodulation of the electrochemical properties, pointing to minimal electronic communication between the pyridinium units. The relatively high reduction potentials of 7 further suggest weak charge delocalization, with the reduced species being electronically localized rather than forming a delocalized radical.

These findings lay the foundation for further exploration of the dual photochromic and electrochromic behaviour of dicationic benzochromenes, offering valuable insights into their fundamental properties and potential applications. However, a more detailed spectroscopic and electrochemical investigation of compounds 6 and 7 is necessary to fully elucidate the complex interplay between their photochromic and electrochromic properties.

Experimental

Unless otherwise stated, reagents and solvents were purchased from major chemical catalogue companies and were used as supplied. For reactions requiring heating, DrySyn® aluminium heating blocks in conjunction with electrical stirrer hotplates were used as the heat source.

Flash column chromatography was performed on chromatography silica gel (either SigmaAldrich, 40 – 63 micron particle size distribution or Fluorochem Silica gel 40 – 63 micron particle

size distribution). All final compounds were homogeneous by TLC using a range of eluent systems of differing polarity [either Merck TLC aluminium sheets silica gel 60 F254 (cat. No 105554) or Fluorochem (cat. No. LC0927)].

Melting points were determined in capillary tubes, using a Stuart SMP10 melting point apparatus, and are uncorrected.

FT-IR spectra were recorded on a Nicolet 380 FTIR spectrophotometer equipped with a diamond ATR attachment (neat sample).

^{1}H NMR, $^{13}C\{^{1}H\}$ NMR, $^{19}F\{^{1}H\}$ NMR, and $^{31}P\{^{1}H\}$ NMR spectra were recorded on a Bruker Avance DPX400 and DPX600 in $CDCl_3$ unless stated otherwise. Chemical shifts are provided in parts per million (ppm) using either the residual solvent peak or TMS as the internal reference. Coupling constants (*J*) are provided in Hz.

Accurate mass measurements were obtained from the Innovative Physical Organic Solutions (IPOS) centre at the University of Huddersfield.

UV-Visible absorption spectra were recorded for acetonitrile or methanol (5% H2O) solutions of the samples (10 mm path length quartz cuvette, PTFE capped, concentration of 10^{-5} mol.dm^{-3}). A bespoke Shimadzu UV-3600 Plus UV-Vis-NIR spectrophotometer was used and equipped with a single cell Peltier temperature controlled (23 °C) magnetically stirred fluorescence cell holder attachment. The spectrophotometer sample chamber door was modified to accept activating irradiation delivered from the light source by liquid light guides (Newport 77557, Newport 77569). An in-line distilled water liquid filter (Newport 6177), multiple filter holder (Newport 62020) and fibre optic coupler (Newport 77799) completed the irradiation equipment. Irradiation was provided by either an ozone-free xenon arc lamp (Newport 6255), powered by a 300-W Oriel power supply (Newport 66906) set to Power Mode 150 W, or a portable LED UV flashlight (Weltool M2-BF 2W, δ_{irr} 365 nm). Activation of the colourless ring-closed forms of the photochromic compounds to their photostationary state was achieved using UV irradiation with: a) the xenon arc lamp (Newport 6255), coupled to a Newport filter (FSQ–UG11, δ_{irr} 325 nm) or b) the LED portable UV flashlight (Weltool M2BF 2W, δ_{irr} 365 nm). The distance between the light sources and cuvettes were kept at 1 cm. In a first experiment, spectra (300 – 700 nm) were recorded prior to (ground state) and immediately after cessation of activating irradiation to a photostationary state. In a second experiment, the decrease of absorbance, Abs, at the wavelength of maximum absorption of the photostationary state, δ_{PSS}, under UV-irradiation was recorded over time (in Kinetic Mode). Bleaching of the coloured (photomerocyanines) when required was affected by irradiation with visible light using an ozone-free xenon arc lamp (Newport 6255), powered by a 300-W Oriel power supply (Newport 66906) set to Power Mode 150 W, coupled to the Newport filter (FSQ–GG420, δ_{irr} > 420 nm). The kinetic data was fitted by employing OriginPro NLFit (ExpDec 1 or ExpDec 2) functions – Iteration Algorithm Levenberg Marquardt.

Emission and excitation spectra were acquired on a Horiba Scientific Fluoromax-4 Spectrophotometer. Emission lifetimes were recorded by time-correlated single-photon counting using an Edinburgh Instruments Mini-Tau spectrometer (EPL-405).

Cyclic voltammograms were recorded using a PalmSens EmStat3 potentiostat with PSTrace electrochemical software. Analyte solutions with a typical concentration of 2 mmoldm-3 were prepared using anhydrous MeCN, freshly distilled over CaH2. All measurements were conducted under an atmosphere of dry N2, employing a glassy carbon working electrode, a Pt wire counter and a leak-free Ag/AgCl reference (Alvatek). Solutions contained nBu4NPF6 as the supporting electrolyte, with a typical concentration of 0.2 moldm-3. Spectroelectrochemical measurements were recorded on an Agilent Cary 60 spectrometer using a quartz cuvette with a pathlength of 0.5 mm (BASi). The working electrode was a Pt gauze (0.5 mm thickness), the counter a Pt wire and the reference was Ag/AgCl, being chemically isolated from the analyte solution by an electrolyte-containing bridge tube tipped with a porous frit. Analyte solutions, of typical concentration 0.4 mmoldm-3, were prepared from freshly distilled dry MeCN and contained 0.2 moldm-3 nBu4NPF6 as supporting electrolyte. Solutions were sparged with dry N2 via a microcapillary and measurements performed under an atmosphere of N2. For spectroelectrochemical studies on the ring-opened species 7, solutions of 6 were first irradiated for 12 minutes with UV light (Weltool M2-BF 2W, δ_{irr} 365 nm), with the UV irradiation maintained throughout the measurements in a direction orthogonal to the beam path of the spectrometer.

Preparation of (4-Bromophenyl) (2,5-dimethoxyphenyl) methanone 10

A stirred solution of 4-bromobenzoic acid (15.00 g, 74.6 mmol) and 1,4-dimethoxybenzene (9.80 g, 70.9 mmol) in polyphosphoric acid (200 g) was heated at 80–90 °C. During this time, additional 1,4-dimethoxybenzene (4.9 g, 35 mmol) was added to the reaction mixture in two portions.† After 8 hours, the reaction mixture was cooled to approximately 35 °C, then diluted with ice (800 g) and left to stand overnight. The resulting mixture was thoroughly stirred and extracted with EtOAc (4 × 75 mL). The combined organic layers were washed with aqueous NaOH solution (3 × 50 mL), followed by water (2 × 100 mL). The organic phase was dried over anhydrous Na2SO4 and the solvent was removed under reduced pressure. The crude product was washed with n-hexane containing ~1% EtOAc, affording the title compound, (4bromophenyl)(2,5-dimethoxyphenyl)methanone (10) as an off-white solid (9.35 g, 39%); mp = 84 – 85 oC (lit. mp = 81 oC [48]); δ_{max} (neat) 3082, 3062, 3008, 2960, 2941, 2901, 2836, 1667, 1582, 1568, 1489, 1469, 1423, 1399, 1309, 1287, 1264, 1237, 1152, 1068, 1044, 1021, 1011, 959, 874, 853, 835, 803, 766, 735, 712, 685, 662, 632, 620, 462 cm-1; 1H NMR (400 MHz, CDCl3) δH 3.66 (3H, s, OMe), 3.79 (3H, s, OMe), 6.91 – 6.94 (2H, m, Ar-H), 7.03 (1H, dd, J = 9.0, 3.1 Hz, Ar-H), 7.57 (2H, app. d, J = 8.6 Hz, Ar-H), 7.67 (2H, app. d, J = 8.6 Hz, Ar-H) ppm; 13C{1H} NMR (100 MHz, CDCl3) δC 55.88, 56.24, 113.01, 114.45, 117.82, 128.13, 128.79, 131.29, 131.55, 136.50, 151.44, 153.56, 195.17 ppm; HRMS observed M+H+ = 321.0117, observed neutral 320.0044, C15H1379BrO3 requires neutral = 320.0048 (mass error = 1.25 ppm).

On heating at 80 – 90 oC the 1,4-dimethoxybenzene sublimes out of the reaction mixture. Synthesis of 1-(4-Bromophenyl)-1-(2,5-dimethoxyphenyl)prop-2-yn-1-ol 11 n-Butyllithium (2.5 M in hexanes, 14.5 mL, 36.2 mmol) was added dropwise via syringe to a cold (-10 °C), stirred solution of trimethylsilylacetylene (4.99 mL, 3.44 g, 35.0 mmol) in anhydrous THF (75 mL) under N_2. After addition, the mixture was stirred at room temperature for 30 minutes. The reaction was then cooled to 0 °C and (4-bromophenyl) (2,5dimethoxyphenyl)methanone (7.50 g, 23.3 mmol) was added in a single portion. The ice bath was removed and the mixture was stirred at room temperature until TLC analysis indicated complete

consumption of the ketone (2 h). The reaction mixture was cooled to 0 °C and a solution of KOH (1.62 g, 24.5 mmol) in MeOH (20 mL) was added in one portion. The cooling bath was removed and stirring continued at room temperature for 1 hour. The reaction was then diluted with water (150 mL) and extracted with EtOAc (3 × 75 mL). The combined organic layers were washed with water (100 mL), dried over anhydrous Na_2SO_4 and evaporated under reduced pressure to afford the title compound, 1-(4-bromophenyl)-1-(2,5-dimethoxyphenyl)prop-2-yn-1-ol (11), as a viscous pale yellow oil (7.90 g, 97%); δmax (neat) 3475, 3286, 2998, 2940, 2834, 1588, 1493, 1485, 1422, 1395, 1361, 1277, 1220, 1178, 1155, 1038, 1010, 943, 880, 842, 810, 735 cm-1; 1H NMR (400 MHz, CDCl3) δH 2.84 (1H, s, acetylene-H), 3.68 (3H, s, OMe), 3.76 (3H, s, OMe), 4.95 (1H, s, OH), 6.81 – 6.87 (2H, m, Ar-H), 7.06 (1H, d, J = 2.6 Hz, Ar-H), 7.39 – 7.46 (4H, m, Ar-H) ppm; 13C{1H} NMR (100 MHz, CDCl3) δC 55.73, 56.41, 73.89, 75.65, 84.93, 113.38, 113.39, 115.16, 121.77, 127.98, 131.13, 132.58, 143.30, 150.68, 153.61 ppm; HRMS observed M+H+-H2O+ = 329.0168, observed neutral 346.0201, C17H1579BrO3 requires neutral = 346.0205 (mass error = 0.16 ppm).

Synthesis of 8-bromo-3-(4-Bromophenyl)-3-(2,5-Dimethoxyphenyl)-3H-Benzo[f]Chromene 12

A solution of 6-bromo-2-naphthol (2.57 g, 11.5 mmol), 1-(4-bromophenyl)-1-(2,5dimethoxyphenyl)prop-2-yn-1-ol (4.0 g, 12 mmol), pyridinium 4-toluenesulfonate (PPTS, 0.14 g, 0.58 mmol) and trimethyl orthoformate (2.45 g, 23 mmol) in 1,2-dichloroethane (100 mL) was heated under reflux for 4 hours, until TLC analysis confirmed the complete consumption of the prop-2-yn-1-ol. The reaction mixture was then cooled to room temperature and the volatiles were removed under reduced pressure, yielding a deep red gum. Purification by silica gel column chromatography (20% EtOAc in light petroleum, bp 40–60 °C) afforded 8-bromo3-(4-bromophenyl)-3-(2,5-dimethoxyphenyl)-3H-benzo[f]chromene (12) as very pale yelloworange microcrystals (4.62 g, 73%); mp = 82 – 83 oC; δmax (neat) 2830, 1633, 1582, 1486, 1421, 1275, 1221, 1180, 1089, 1070, 1044, 1001, 961, 879, 804, 772, 734, 672, 555, 460 cm-1; 1H NMR (400 MHz, d6-AcMe) δH 3.54 (3H, s, OMe), 3.72 (3H, s, OMe), 6.63 (1H, d, J = 10.1 Hz, 2-H), 6.85 (1H, dd, J = 8.9, 3.1 Hz, Ar-H), 6.93 (1H, d, J = 8.9 Hz, Ar-H), 7.30 (1H, d, J = 8.9 Hz, 5H), 7.36 (1H, d, J = 3.1 Hz, Ar-H), 7.40 – 7.42 (3H, m, Ar-H, 1-H), 7.45 – 7.48 (2H, m, Ar-H), 7.58 (1H , dd, J = 9.0, 2.1 Hz, 9-H), 7.75 (1H, d, J = 8.9 Hz, 6-H), 8.01 (1H, d, J = 2.0 Hz, 7-H), 8.04 (1H, d, J = 9.1 Hz, 10-H) ppm; 13C{1H} NMR (100 MHz, d6-AcMe) δC 54.92, 55.44, 81.30, 112.86, 113.49, 113.74, 114.45, 117.04, 118.89, 119.30, 121.00, 123.78, 127.01, 128.32, 128.99, 129.22, 129.72, 130.33, 130.73, 130.77, 132.73, 143.36, 149.50, 150.39, 153.76 ppm; HRMS observed M+H+ = 550.9807 (2 × 79Br), 552.9818 (79Br & 81Br), observed neutral 549.9760 (2 × 79Br), C27H2079BrO3 requires neutral = 549.9779 (mass error 3.45 ppm).

Preparation of 4-(3-(2,5-Dimethoxyphenyl)-3-(4-(Pyridin-4-yl) phenyl)-3H-benzo[f]chromen8-yl) pyridine 14

A stirred suspension of 8-bromo-3-(4-bromophenyl)-3-(2,5-dimethoxyphenyl)-3Hbenzo[f]chromene (3.00 g, 5.43 mmol), 4-(4,4,5,5-tetramethyl-1,3,2-dioxaborolan-2yl)pyridine (3.34 g, 16.3 mmol) and potassium fluoride (1.26 g, 21.7 mmol) in a 1:1 mixture of EtOH and PhMe (90 mL) was bubbled with N2 for 30 minutes. Pd(PPh3)4 (0.38 g, 0.33 mmol, 6 mol%) was then added, and the reaction mixture was heated under reflux under N2 for 22 hours, until TLC analysis indicated no further reaction. After cooling, the mixture was diluted with water (250 mL) and extracted with EtOAc (4 × 50 mL). The combined organic layers were washed with water (2 × 100 mL), dried over anhydrous Na2SO4 and concentrated under reduced pressure to yield the crude product as an orange foam. Purification by silica gel chromatography (eluting with 70% EtOAc in n-hexane, gradually increasing to 40% MeOH in EtOAc) afforded two fractions. Fraction 1: 4-(3-(4-bromophenyl)-3-(2,5-dimethoxyphenyl)3H-benzo[f] chromen-8-yl)pyridine (13) as a pale pink powder 0.66 g (22%); mp = 171 – 174 oC; □max (neat) 2991, 2833, 1627, 1586, 1547, 1496, 1462, 1441, 1412, 1286, 1246, 1223, 1199, 1170, 1087, 1043, 1006, 962, 898, 861, 824, 810, 773, 739, 721, 665, 591, 511, 485, 466 cm-1;

1H NMR (400 MHz, CDCl3) □H 3.51 (3H, s, OMe), 3.76 (3H, s, OMe), 6.53 (1H, d, J = 10.1 Hz, 2H), 6.80 – 6.81 (2H, m, Ar-H), 7.22 (1H, d, J = 8.8 Hz, 5-H), 7.29 (1H, d, J = 10.1 Hz, 1-H), 7.32 – 7.35 (2H, m, Ar-H), 7.38 – 7.41 (3H, m, Ar-H), 7.59 – 7.61 (2H, m, Py-H), 7.73 – 7.76 (2H, m, ArH), 8.00 (1H, d, J = 2.0 Hz, 7-H), 8.06 (1H, d, J = 8.9 Hz, 10-H), 8.67 – 8.69 (2H, m, Py-H) ppm; 13C{1H} NMR (100 MHz, CDCl3) δC 55.69, 56.11, 81.54, 113.03, 113.61, 113.87, 113.96, 118.99, 119.03, 121.56, 121.62, 122.49, 125.19, 126.49, 127.00, 128.96, 129.45, 129.82, 130.29, 130.92, 132.98, 133.13, 143.00, 148.06, 149.53, 150.31, 150.85, 153.65 ppm; HRMS observed M+H+ = 550.1014, observed neutral 549.0936, C32H2479BrNO3 requires neutral = 549.0940 (mass error 0.73 ppm). Fraction 2: 4-(3-(2,5-dimethoxyphenyl)-3-(4-(pyridin-4-yl)phenyl)-3Hbenzo[f]chromen-8-yl)pyridine (14) as a cream solid 0.87 g (29%) after a hot wash with nhexane and acetone; mp = 189 – 192 oC; δmax (neat) 2981, 1633, 1595, 1547, 1486, 1460, 1422, 1277, 1223, 1183, 1171, 1151, 1086, 1052, 1025, 1000, 972, 879, 825, 808, 792, 741, 717, 664, 599, 548, 522, 487 cm-1; 1H NMR (400 MHz, DMSO-d6) δH 3.52 (3H, s, OMe), 3.67 (3H, s, OMe), 6.66 (1H, d, J = 10.1 Hz, 2-H), 6.86 (1H, dd, J = 8.9, 3.0 Hz, Ar-H), 6.97 (1H, d, J = 8.9 Hz, Ar-H), 7.25 (1H, d, J = 3.0 Hz, Ar-H), 7.36 (1H, d, J = 8.8 Hz, Ar-H), 7.49 – 7.53 (3H, m, 1-H, Ar-H), 7.65 (2H, d, J = 6.0 Hz, Py-H), 7.74 (2H, d, J = 8.4 Hz, Ar-H), 7.82 (2H, d, J = 6.0 Hz, Py-H), 7.90 – 7.94 (2H, m, Ar-H), 8.22 (1H, d, J = 8.9 Hz, Ar-H), 8.31 – 8.33 (1H, m, Ar-H), 8.59 (2H, d, J = 5.9 Hz, Py-H), 8.64 (2H, d, J = 5.9 Hz, Py-H) ppm; 13C{1H} NMR (150 MHz, DMSO-d6) δC 55.79, 56.60, 81.66, 113.31, 113.83, 114.22, 114.58, 119.18, 119.48, 121.57, 121.64, 123.27, 125.69, 126.91, 127.31, 127.74, 128.08, 129.63, 129.85, 131.14, 132.75, 132.81, 136.81, 144.90, 146.48, 146.93, 147.04, 149.70, 150.67, 150.74, 150.88, 153.51 ppm; HRMS observed M+H+ = 549.2168, neutral 548.2095, C37H28N2O3 requires neutral = 548.2100 (mass error 0.91 ppm).

Preparation of 4-(3-(2,5-dimethoxyphenyl)-3-(4-(1-hexylpyridin-1-ium-4-yl)phenyl)-3Hbenzo[f]chromen-8-yl)-1-hexylpyridin-1-ium bis(hexafluorophosphate) 6

1-Iodohexane (0.67 mL, 0.97 g, 4.6 mmol) was added in a single portion via syringe to a stirred suspension of 4-(3-(2,5-dimethoxyphenyl)-3-(4-(pyridin-4-yl)phenyl)-3H-benzo[f]chromen-8yl)pyridine (0.50 g, 0.90 mmol) in anhydrous acetonitrile (15 mL). The flask was wrapped in foil to protect from light and heated under reflux for 24 hours. The resulting brown solution was cooled to room temperature, diluted with diethyl ether (30 mL), and the precipitate collected by vacuum filtration. The solid was washed with diethyl ether and air-dried to afford the intermediate 4-(3-(2,5-dimethoxyphenyl)-3-(4-(1-hexylpyridin-1-ium-4-yl)phenyl)-3Hbenzo[f]chromen-8-yl)-1-hexylpyridin-1-ium diiodide (0.63 g, 71%). A solution of this diiodide (0.20 g, 0.20 mmol) in warm methanol (ca. 40 °C, 20 mL) was added dropwise through a glass wool-plugged Pasteur pipette to a stirred solution of ammonium hexafluorophosphate (3.92 g, 24 mmol)

in water (20 mL). The mixture was stirred for 30 minutes. The resulting fine yellow precipitate was filtered, washed with water (3 × 5 mL) and air-dried to yield 4-(3-(2,5dimethoxyphenyl)-3-(4-(1-hexylpyridin-1-ium-4-yl)phenyl)-3H-benzo[f]chromen-8-yl)-1hexylpyridin-1-ium bis(hexafluorophosphate) (6) as a bright yellow powder (0.20 g, 95%); mp = not discernible, at 150 oC sample becomes mustard coloured, brown by 199 oC and black by 220 oC (decomp.); δmax (neat) 2931, 2860, 1637, 1611, 1524, 1496, 1463, 1384, 1244, 1223, 1171, 1092, 1042, 1004, 966, 825, 739, 555 cm-1; 1H NMR (600 MHz, d6-AcMe) δH 0.877 (3H, t, J = 7.2 Hz, CH3), 0.895 (3H, t, J = 7.2 Hz, CH3), 1.28 – 1.53 (12H, m, CH2), 2.10 – 2.23 (4H, m, CH2), 3.60 (3H, s, OMe), 3.78 (3H, s, OMe), 4.81 – 4.86 (4H, m, N+-CH2), 6.79 (1H, d, J = 10.1 Hz, 2-H), 6.92 (1H, dd, J = 8.8, 3.1 Hz, Ar-H), 7.02 (1H, d, J = 8.9 Hz, Ar-H), 7.44 (1H, d, J = 3.1 Hz, Ar-H), 7.48 (1H, d, J = 8.9 Hz, 5-H), 7.59 (1H, d, J = 10.1 Hz, 1-H), 7.80 (2H, app. d, J = 8.6 Hz, Ar-H), 8.03 – 8.06 (3H, m, Ar-H), 8.19 (1H, dd, J = 8.8, 2.0 Hz, 9-H), 8.40 (1H, d, J = 8.9 Hz, 10-H), 8.54 (2H, app. d, J = 7.1 Hz, Py-H), 8.68 – 8.70 (3H, m, Py-H, 7-H), 9.16 (2H, app. d, J = 7.1 Hz, Py-H), 9.18 (2H, app. d, J = 7.0 Hz, Py-H) ppm; 19F{1H} NMR (376 MHz, d6-AcMe) δF 72.50 (d, J = 707 Hz) ppm; 31P{1H} NMR (162 MHz, d6-AcMe) δP -144.26 (d, J = 707 Hz) ppm; 13C{1H} NMR (150 MHz, d6-AcMe) δC 13.25, 13.28, 22.12, 22.15, 25.50, 25.55, 30.95, 30.98,
31.10, 31.13, 55.01, 55.52, 61.00, 61.11, 81.73, 113.07, 113.70, 113.91, 114.46, 119.08, 119.61, 123.51, 124.67, 124.94, 125.05, 127.00, 127,75, 128.42, 129.03, 129.48, 129.91,
131.38, 131.57, 132.44, 133.11, 144.62, 144.71, 148.24, 149.59, 152.36, 153.89, 155.75, 155.85 ppm; HRMS observed M-2(PF6-)2+ = 359.2062, observed neutral [-2(PF6-)] 718.4134, C49H54F12N2O3P2 requires neutral [-2(PF6-)] = 718.4134, (mass error 0 ppm).

Acknowledgement
The authors are indebted to Dr Stuart Aiken who spent many tireless hours processing and evaluating the many NMR spectra required to establish the structure of the molecules reported herein. The University of Huddersfield is thanked for financial support to Dr Orlando D. C. C. De Azevedo.

References

1. Weigand U, Zinner H (2018) PCT Int. Appl. WO2018/054507.
2. He M, Mondal S, Dabideen DR, Kumar A, Dai X-M (2012) PCT Int. Appl., WO2012/082383.
3. Aiken S, Gabbutt CD, Heron BM, Kershaw CS, Smith NJ, et al. (2009) PCT Int. Appl, WO2009/109546.
4. Clarke DA, Heron BM, Bernard, Hepworth JD, Partington SM, et al. (1998) PCT Int. Appl, WO1998/42693.
5. Izumi S, Shimizu Y, Momoda J (2013) PCT Int. Appl, WO2013/141143.
6. Chan YP, Bryson N (1998) PCT Int. Appl, PCT WO1998/04937.
7. Hepworth JD, Heron BM (2006) In: 'Functional Dyes', ed. S-H. Kim, Elsevier (Amsterdam): 85-135.
8. Van Gemert B (1998) In Organic Photochromic and Thermochromic Compounds, Main Photochromic Families; eds. J. C. Crano, R. J. Guglielmetti, Plenum Press (New York) 1: 111-140.
9. Mukhopadhyay A, Moorthy JN, Photochem J. Photobiol (2016) C: Photochemistry Reviews 29: 73-106.
10. (a) Azevedo ODCC De, Elliott PIP, Gabbutt CD, Heron BM, Scattergood PA (2025) Exploring a Dicationic Benzochromene with Dual Photochromic and Electrochromic Response. SSRN 242: 112998. (b) De Azevedo ODCC, Elliott PIP, Gabbutt CD, Heron BM, Jacquemin D, et al. (2021) Quenching of the phosphorescence of thermally reversible photochromic naphthopyran Re(i) complexes initiated by either visible or ultraviolet radiation. Dalton Trans 50: 830-834.
11. Paramonov SV, Lokshin V, Smolentsev AM, Glebov EM, Korolev VV, et al. (2012) Tetrahedron 68: 7873-7883.
12. Fedorova OA, Maurel F, Chebun'kova AV, Strokach Yu P, Valova TM, et al. (2007) Investigation of cation complexation behavior of azacrown ether substituted benzochromene. J Phys Org Chem 20: 469-483.
13. Ushakov EN, Nazarov VB, Fedorova OA, Gromov SP, Chebun'kova AV, et al. (2003) Photocontrol of Ca2+ complexation with an azacrown-containing benzochromene. J Phys Org Chem 16: 306-309.
14. Fedorova OA, Maurel F, Ushakov EN, Nazarov VB, et al. (2003) Synthesis, photochromic behaviour and light-controlled complexation of 3,3-diphenyl-3H-benzo[f] chromenes containing a dimethylamino group or an aza-15-crown-5 ether unit. New J Chem 27: 1720-1730.
15. Gabbutt CD, Heron BM, Kolla SB, Mcgivern M (2008) Two Stage Colour Modulation of Triarylmethine Dyes Derived from a Photochromic Naphthopyran. Eur J Org Chem 20312034.
16. Aiken S, Clayton D, Gabbutt CD, Heron BM, Kolla SB (2013) Cationic merocyanine dyes by photomodulation of [4-(naphthopyran-3-yl) phenyl] methines. Dyes Pigm 97: 118123.
17. Kahle I, Tröber O, Richter H, Spange S (2013) Synthesis and optical properties of naphthopyran dyes conjugated with fluorescent stilbazolium moieties. New J Chem 37: 1479-1485.
18. Aiken S, Armitage GK, Azevedo ODCC de, Crossley DL, Dobson R, et al. (2022) 2, 2, 4, 6-Tetraaryl-2H-benzo [h] chromenes: The influence of electronic communication between aryl substituents on their photochromism. Dyes Pigm 199: 110036.
19. Aiken S, Booth K, Gabbutt CD, Heron BM, Rice CR, et al (2014) The first structural and spectroscopic characterisation of a ring-opened form of a 2H-naphtho[1,2-b]pyran: a novel photomerocyanine. A Chem Commun 50: 7900-7903.
20. Gabbutt CD, Heron BM, Instone AC, Thomas DA, Partington SM, et al. (2003) Observations on the Synthesis of Photochromic Naphthopyrans. Eur J Org Chem 2003: 1220-1230.
21. Clarke DA, Heron BM, Gabbutt CD, Hepworth JD, Partington SM (2000) PCT Int. Appl WO 2000/018755,
22. Aiken S, Cano J-P, Gabbutt CD, Heron BM, Patent US (2013) US8 436:184.
23. de Azevedo ODCC, Elliott PIP, Gabbutt CD, Heron BM, Lord KJ, et al. (2020) Synthesis and Photochromism of Novel Pyridyl-Substituted Naphthopyrans. J Org Chem 85: 10772-10796.
24. Biver C, Berit-Debat F, Archambeau S, Aiken S, Armitage GK, et al. (2022) PCT Int. Appl WO 2022/136020.
25. Biver C, Berit-Debat F, Archambeau S, Gabbutt CD, Aiken S, et al. (2018) PCT Int Appl WO 2018/127540.
26. Gilat SL, Kawai SH, Lehn JM (1995) Light-Triggered Molecular Devices: Photochemical Switching Of optical and Electrochemical Properties in Molecular Wire Type Diarylethene Species. Chem Eur J 1: 275-284.
27. Gorodetsky B, Branda NR (2007) Bidirectional Ring-Opening and Ring-Closing of Cationic 1,2-Dithienylcyclopentene Molecular Switches Triggered with Light or Electricity. Adv Funct Mater 17: 786-796.

28. Khettabi A, Grempka A, Lafolet F, Chatir E, Leconte N, et al. (2020) Catalytic Light-Triggered Reduction Promoted by a Dithienylethene Derivative. Chem Eur J 26: 13359-13362.
29. Sicard L, Lafolet F, Boggio-Pasqua M, Bucher C, Royal G, et al. (2022) New Insights into the Redox Properties of Pyridinium Appended 1,2-Dithienylcyclopentenes. Chem Phys Chem 23: e202200004.
30. Ding J, Zheng C, Wang L, Lu C, Zhang B, et al. (2019) Viologen-inspired functional materials: synthetic strategies and applications. Chem A 7: 23337-23360.
31. Neira I, Blanco-Gómez A, Quintela JM, García MD, Peinador C (2020) Dissecting the "Blue Box": Self-Assembly Strategies for the Construction of Multipurpose Polycationic Cyclophanes. Acc Chem Res 53: 2336-2346.
32. Monk PMS, Rosseinsky RJ (2015) Electrochromic Materials and Devices, ed Mortimer, Wiley-VCH (Weinheim) chapter 3: 57-89.
33. Gabbutt CD, Heron BM, Instone AC (2003) Control of the fading properties of photochromic 3,3-diaryl-3H-naphtho[2,1-b]pyrans. Heterocycles 60: 843-855.
34. Aiken S, Azevedo ODCC de, Chauhan K, Driscoll T, Elliott PI, et al. (2020) Base-Mediated Ring-Contraction of Pyran Systems Promoted by Palladium and Phase-Transfer Catalysis. J Org Chem 85: 952-966.
35. Gabbutt CD, Heron BM, Kolla SB, Kilner C, Coles SJ, et al. (2008) Ring contraction during the 6π-electrocyclisation of naphthopyran valence tautomers. Org Biomo Chem 6: 3096-3104.
36. Demadrille R, Moustrou C, Samat A, Guglielmetti R (1999) PALLADIUM-CATALYZED AMINATION OF PHOTOCHROMIC TRIFLATE-SUBSTITUTED 3H-NAPHTH0 [1, 2-b] PYRANS. Heterocycl Commun 5: 123-126.
37. Lin J, Van Gemert B (1999) PCT Int Appl WO 1999/31082.
38. Gabbutt CD, Gelbrich T, Hepworth JD, Heron BM, Hursthouse MB, et al. (2002) Synthesis and photochromic properties of some fluorine-containing naphthopyrans. Dyes Pigm 54: 79-93.
39. Bird CL, Kuhn MT (1981) Electrochemistry of the viologens. Chem Soc Rev 10: 49-82.
40. Takahashi K, Nihira T, Akiyama K, Ikegami Y, Fukuyo E (1992) Synthesis and characterization of new conjugation-extended viologens involving a central aromatic linking group. J Chem Soc Chem Commun: 620-622.
41. Ebbesen TW, Akaba R, Tokumaru K, Washio M, Tagawa S, et al. (1988) Cis and trans olefin radicals: equilibrium and photoisomerization. J Am Chem Soc 110: 2147-2151.
42. Sayre LM, Arora PK, Feke SC, Urbach FL (1986) Mechanism of induction of Parkinson's disease by 1-methyl-4-phenyl-1,2,3,6-tetrahydropyridine (MPTP). Chemical and electrochemical characterization of a geminal-dimethyl-blocked analog of a postulated toxic metabolite. J Am Chem Soc 108: 24642466.
43. Archambeau S, Biver C, Berit-Debat F, Aiken S, Gabbutt CD, et al. (2017) PCT Int Appl WO 2017/005824.
44. Fortage J, Peltier C, Perruchot C, Takemoto Y, Teki YF, et al. (2012) Tictoid Expanded Pyridiniums: Assessing Structural, Electrochemical, Electronic, and Photophysical Features. J Am Chem Soc 134: 2691-2705.
45. Hirao Y, Taniguchi T, Teraoka M, Kubo T (2019) Redox/pH Dual Stimuli-Responsive Acridine Spiropyran. Asian J Org Chem 8: 863-866.
46. Mendive-Tapia D, Kortekaas L, Steen JD, Perrier A, Lasorne B, et al. (2016) Accidental degeneracy in the spiropyran radical cation: charge transfer between two orthogonal rings inducing ultra-efficient reactivity. Phys Chem 18: 31244-31253.
47. JD Steen, Duijnstee DR, Sardjan AS, Martinelli J, Kortekaas L, et al. (2021) Electrochemical Ring-Opening and -Closing of a Spiropyran. J Phys Chem A 125: 3355-3361.
48. Waterlot C, Hasiak B, Couturier D, Rigo B (2001) Tetrahedron 57: 4889-4901.